

Influence of soil type on chemiresistive detection of buried ANFO

Merel J. Lefferts^{*}, Martin R. Castell

Department of Materials, University of Oxford, Parks Road, Oxford OX1 3PH, UK

ARTICLE INFO

Keywords:

Chemiresistor
Vapour sensor
Conducting polymer
ANFO
Buried
Soil

ABSTRACT

Ammonium nitrate/fuel oil (ANFO) is one of the most commonly used materials for improvised explosive devices (IEDs). Stand-off ANFO vapour sensors that are small, inexpensive, and easy to use will allow for the detection of IEDs in security and humanitarian settings. Concealment is one of the main challenges of IED detection and increases the need for highly sensitive vapour sensors. Here, percolation networks of polypyrrole (PPy) are used to detect ANFO buried under various types of soil. Percolation networks are used to achieve an improved sensitivity compared to thin film-based vapour sensors, achieving a limit of detection of 73 ± 11 ppbv NH_3 . The influence on the sensor response of concealment under different soil types, as well as the thickness of the soil layer, is investigated. Reliable detection of ANFO buried under layers of sand or sandy soil is demonstrated at sub-ppm concentrations, however clay is found to act as a significant barrier to the permeability of NH_3 .

Introduction

The detection of improvised explosive devices (IEDs) is important for both security and humanitarian applications. Cheap and reliable humanitarian demining remains a challenge, especially in developing countries where unexploded devices remain concealed due to past or present conflicts. Typically, IEDs are based on materials that are easily available, such as perchlorates or a mixture of ammonium nitrate and fuel oil (ANFO) [1]. The detection of ANFO is especially challenging because ammonium nitrate (AN) itself is not volatile, although its decomposition products NH_3 and HNO_3 are [2,3].

Although sniffer dogs are still the gold standard in terms of sensitivity, it is not always practical to use dogs for explosives detection. Established technological solutions, such as methods based on mass spectrometry [4], often rely on large pieces of equipment that are expensive and not practical for the detection of IEDs in the field. Furthermore, metal detectors, ground penetrating radar, acoustic sensors, and other methods that are traditionally used for the detection of mines can be ineffective because of the large range of materials, shapes, and sizes of the containers used for IEDs [5]. Conducting polymer (CP) based chemiresistive sensors offer a potential solution because they are small, easy to use, relatively inexpensive, and can operate at room temperature [6]. Sensors based on CPs have been demonstrated for a large range of sensing and analyte materials [7–12]. Recent work has demonstrated ppbv level ANFO vapour sensing using percolation networks of polypyrrole (PPy) [13]. NH_3 , one of the decomposition

products of ammonium nitrate, is a strong electron donor and upon interaction causes an increase in the resistance of p-type PPy. It has been shown that by using a percolation network of conductive polymers, instead of a more traditional thin film, it is possible to significantly increase the sensitivity. Close to the percolation threshold an interaction with an analyte molecule has a larger effect on the resistance of the polymer layer as a whole, compared to an interaction with a polymer film, resulting in a more sensitive sensor [14].

However, detection of buried IEDs remains a challenge. The performance of all sensors is affected by both the presence and the properties of the soil under which the IED is buried [15]. Gas permeability is related to the texture and bulk density of the soil and is therefore different for different soil types [16]. One recent example for stand-off detection of buried mines uses an optical biosensor [17,18]. Although promising, this method relies on bacterial beads placed on the soil surface, introducing the additional challenge of removing or deactivating the beads after testing the area for the presence of mines. Another recent example uses a Super Yellow-based system placed directly over the sample for optical detection of 2,4-dinitrotoluene (DNT) and 2,4,6-trinitrotoluene (TNT) [19].

The additional challenges posed by concealment highlight the need for highly sensitive sensors for stand-off explosives detection and the importance of understanding the impact of the soil layer on the sensor performance for buried IEDs. Here we demonstrate chemiresistive vapour sensing using PPy percolation networks of ANFO concealed under a layer of soil. The effects of soil type and soil layer thickness on

^{*} Corresponding author.

E-mail address: merel.lefferts@materials.ox.ac.uk (M.J. Lefferts).

<https://doi.org/10.1016/j.forc.2022.100401>

Received 9 November 2021; Received in revised form 20 January 2022; Accepted 21 January 2022

Available online 25 January 2022

2468-1709/© 2022 The Authors. Published by Elsevier B.V. This is an open access article under the CC BY license (<http://creativecommons.org/licenses/by/4.0/>).

Table 1

Overview of soil types used and their composition, classification, and visual appearance. Clay particles are defined as being smaller than 3.9 μm , sand particles as larger than 62.5 μm , and silt as the intermediate between clay and sand [23].

	Clay	Sand	Silt	Classification	Visual appearance
Sandy soil #1	3.3%	93.3%	3.3%	Sand	Granular
Clean sand #4	1.0%	98%	1.0%	Sand	Granular
Clean clay #5	95%	3.5%	1.5%	Clay	Fine powder

the sensor response are also investigated.

Methods

Sensor fabrication

Pt interdigitated electrodes (IDEs) with a 5 μm electrode separation on glass substrates (Micrux, Spain) were used after cleaning with concentrated nitric acid (HNO_3 , 90%, Merck), followed by sonication in ethanol ($\text{C}_2\text{H}_6\text{OH}$, 99.8%, Merck), methanol (CH_3OH , 99.9%, Merck), and acetone ($\text{C}_3\text{H}_6\text{O}$, 99.8%, Merck). Electrochemical polymerisation from a solution of 0.01 M pyrrole (Merck) and 0.1 M lithium perchlorate (LiClO_4 , Merck) in acetonitrile ($\text{C}_2\text{H}_3\text{N}$, Merck) was used to grow polypyrrole (PPy). A 3-electrode set-up was used. The IDEs were electrically connected together and used as the working electrode. An Ag/AgCl (CH Instruments, USA) reference electrode and a Pt coil (BASi, USA) counter electrode were used. The electrochemical polymerisation was monitored and controlled via an Autolab PGSTAT204 potentiostat (Metrohm, Switzerland) and a PC with Nova 1.11 software [20]. Chronoamperometry was used to keep the potential between the working electrode and the reference electrode at 1.0 V for 60 s. This typically resulted in sensors with a starting resistance between 5 k Ω and 50 k Ω . From previous work on PPy deposition between Au IDEs on flexible PET substrates we know that this corresponds to the percolation region for PPy networks [14]. Finally, the sensors were p-doped in a monomerless 0.1 M LiClO_4 solution, using chronoamperometry at 1.0 V for 60 s. Electrochemical polymerisation was used for the growth of PPy networks because this method allows for a high level of control and the formation of networks with sub-thin film polymer coverage. However, due to the random nature of electrochemical polymerisation, resulting polymer networks and their electrical resistance can vary even when they are produced in the same way. This is a significant challenge that needs to be addressed before electrochemically grown sensors can be produced at a large scale.

Buried AN(FO) detection

The sensors were exposed to vapour emitted by crushed Nutribooster (YaraBela UK) and crushed Nutribooster mixed with diesel (Merck). The nitrogen content of Nutribooster is 25%, of which half is nitrate-N and half ammoniacal-N. Each ANFO sample consisted of ~ 0.94 g Nutribooster and 0.06 mL diesel because this is the ratio most commonly used in IEDs [21,22]. Exposures to 1–8 ppm NH_3 (from a 10 ppm NH_3 in N_2 cylinder, BOC) were used to calibrate the sensors. N_2 (zero grade, BOC) was used to carry vapours emitted by the fertiliser and ANFO samples into the sensing chamber and to further dilute the NH_3 . To allow for a comparison of sensor signals from samples below thicker or less permeable soil layers, the exposure time was set at 5 min. However, because of the fast sensor responses, shorter exposure times that are more suitable for practical implementation are sufficient for normal sensor operation. For safety reasons, the sample size was limited to 1 g for all fertiliser and ANFO samples. Furthermore, fertilisers and fuel oils were stored separately, and AN(FO) waste was kept in an excess of water for disposal.

The fertiliser and ANFO samples were covered by up to 1 g of clean

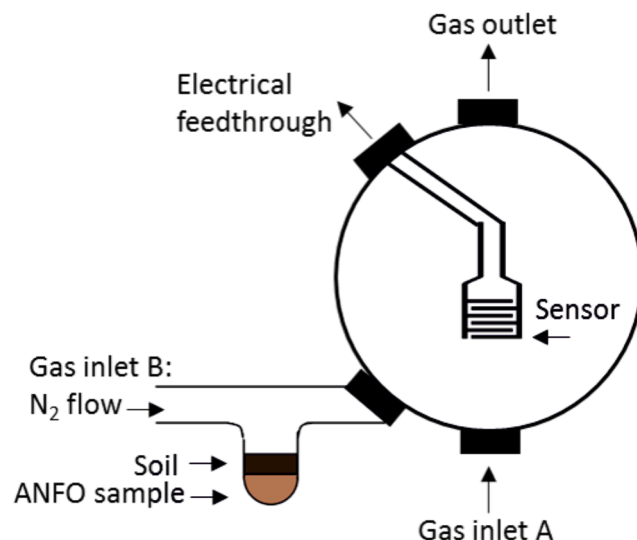


Fig. 1. Schematic representation of the sensing chamber, showing gas inlets and outlet and the T-shaped attachment containing an ANFO sample covered by a layer of soil. (Adapted from Lefferts et al. [13]).

sandy soil #1, clean sand #4, and clean clay #5 (Merck, Table 1). The soil was used as received and placed on top of the ANFO samples without excessive packing.

A custom-made sensor testing chamber was used to test the sensors at atmospheric pressure and room temperature (Fig. 1). A constant flow rate of 500 sccm was maintained using mass flow controllers (Alicat). The custom-made sensing chamber has 2 gas inlets and 1 gas outlet. Gas inlet A is used for N_2 and mixtures of N_2 and NH_3 from gas cylinders. Inlet B has a T-shaped glass attachment that is used to hold liquid and solid samples such as the fertiliser, ANFO, and soil samples. N_2 is used to carry vapours emitted by the fertiliser, ANFO, and/or soil sample held in the T-shaped attachment into the sensor testing chamber through gas inlet B. Between exposures the T-shaped attachment is cleaned and the fertiliser, ANFO, and/or soil sample is exchanged. Between exposures the continuous N_2 flow through the sensor testing chamber is maintained by switching the N_2 flow from gas inlet B to gas inlet A. The changes in the resistance of the sensor were monitored during exposure to the analytes by applying 1.0 V to the sensor and measuring the current.

Results and discussion

PPy percolation network sensors were fabricated and placed under N_2 flow in the sensor testing chamber for 20 min to remove any impurities. First, a control experiment was conducted by flowing the N_2 carrier gas through the empty T-shaped attachment. Next, 1 g of either clay, sandy soil, or sand was placed in the T-shaped attachment and the sensor was exposed to vapours emitted by the soil sample and carried into the chamber by N_2 for 5 min. This was to ensure that the soil samples did not emit any vapours that cause a sensor response. Then, a series of 5 min exposures to either 1 g crushed fertiliser or 1 g ANFO, consisting of 0.94 g crushed fertiliser and 0.06 mL diesel, covered by 1 g, $\frac{1}{2}$ g, and $\frac{1}{4}$ g of soil were conducted. 1 g fertiliser or ANFO corresponds to a layer thickness of 12 mm, measured at the deepest point of the round bottomed sample holder. Sand or sandy soil layers of 1 g, $\frac{1}{2}$ g, and $\frac{1}{4}$ g correspond to a depth of 6 mm, 3 mm, and 1.5 mm respectively, whereas 1 g, $\frac{1}{2}$ g, and $\frac{1}{4}$ g of clay correspond to a depth of 9 mm, 4.5 mm, and 2.25 mm respectively. It should be noted that while these quantities can be weighed to a high level of precision, the measured depths are approximate as a result of grain size, irregular surfaces, and mixing at the interface between the fertiliser and the soil. Each series of exposures was completed with an exposure to an AN(FO) sample without a soil

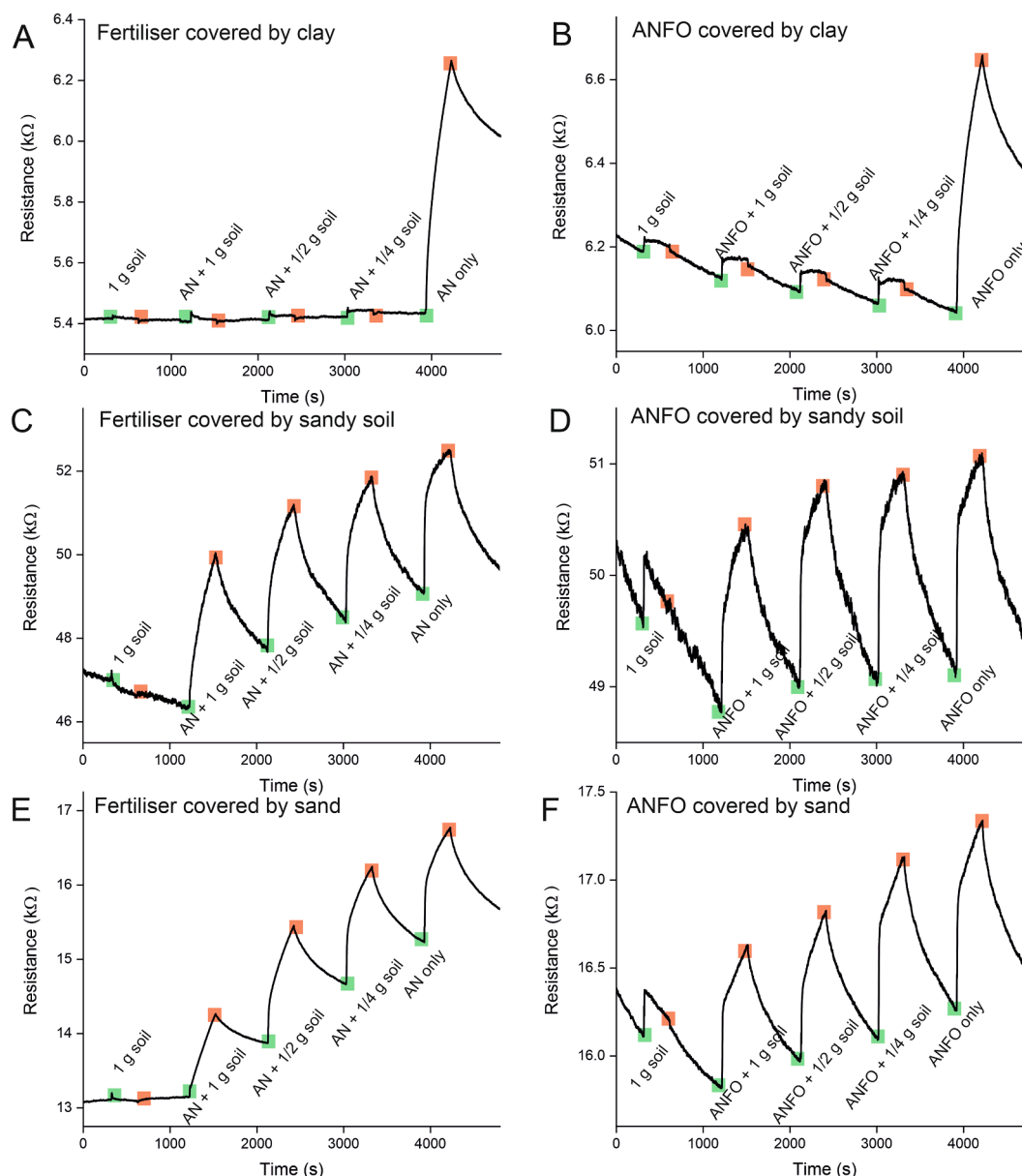


Fig. 2. Sensor responses to fertiliser and ANFO respectively, covered by clay (A and B), sandy soil (C and D), and sand (E and F). Each series of exposures consists of 5 consecutive 5 min exposures to 1 g soil, 1 g fertiliser or ANFO covered by 1 g soil, 1 g fertiliser or ANFO covered by $\frac{1}{2}$ g soil, 1 g fertiliser or ANFO covered by $\frac{1}{4}$ g soil, and 1 g fertiliser or ANFO without soil layer. The sensor response is an increase in resistance and is reversed during the 10 min recovery time under N_2 flow. Green indicates the start of an exposure to vapour emitted by the fertiliser, ANFO, and/or soil sample and red indicates the start of the recovery phase under N_2 flow. (For interpretation of the references to colour in this figure legend, the reader is referred to the web version of this article.)

layer. The sensor was left to recover under N_2 flow for 10 min between exposures (Fig. 2). The AN(FO) causes a reversible increase in resistance. Although ammonium nitrate itself is not volatile, it decomposes into NH_3 and HNO_3 [2,3]. NH_3 is a strong electron donor and its interaction with p-type PPY causes a decrease in the majority charge carriers, increasing the resistance of the PPY network. This is in agreement with previous work [13]. Although previous work has shown that the sensor response to (AN)FO is not consistent with a sensor response to NO_2 [13], for completeness future work should also test the sensor response to HNO_3 .

AN(FO) samples buried under clay (Fig. 2A and 2B) result in an almost negligible sensor response for both 1 g, $\frac{1}{2}$ g, and $\frac{1}{4}$ g of clay. This is perhaps surprising because $\frac{1}{4}$ g of soil results in a very thin layer and is barely enough to cover the entire AN(FO) sample. On the other hand, AN(FO) samples covered by sandy soil (Fig. 2C and 2D) and sand (Fig. 2E

and 2F) caused a significant sensor response. For Fig. 2B, 2D, and 2F the step at the start of the first exposure, to just the soil, is due to a small amount of vapour still present in the tubes of the setup and does not result in a resistance increase for the rest of the 5 min duration of the exposure. The negative slope of the baseline in Fig. 2B is likely due to ongoing recovery of a previous exposure to a large vapour concentration. Although the sensor response is somewhat decreased with increasing thickness of the sandy soil or sand layer, all AN(FO) samples covered by sandy soil and sand were comfortably within the limit of detection of our sensors. The difference in sensor response for AN(FO) concealed by clay, sandy soil, and sand can be explained by the properties of the different soil types, and is consistent with literature on gas permeability of soil [16]. Clay is defined as consisting of particles smaller than $3.9 \mu m$ and sand as larger than $62.5 \mu m$, with silt being the intermediate [23]. The small clay particles form a compact layer that is

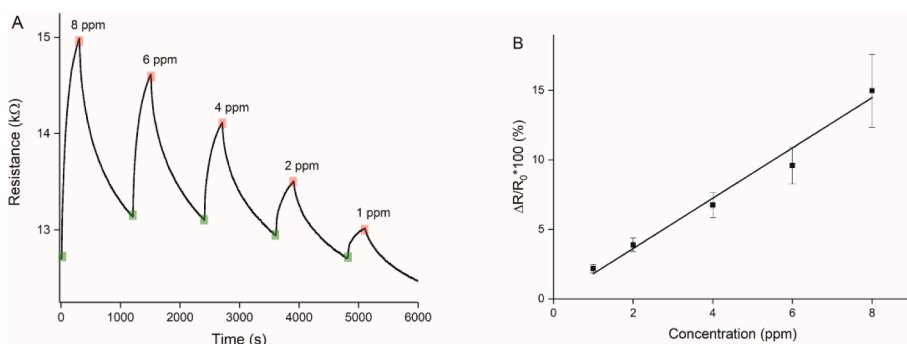


Fig. 3. (A) Typical response of a PPy percolation network sensor to consecutive 5 min exposures of 8, 6, 4, 2, and 1 ppm NH_3 . The sensor was left to recover under N_2 flow for 15 min between NH_3 exposures. Green indicates the start of a exposure to NH_3 and red indicates the start of the recovery phase under N_2 flow. (B) Calibration plot based on 3 exposures per NH_3 concentration. The error bars represent the standard deviation of the 3 exposures for each concentration. (For interpretation of the references to colour in this figure legend, the reader is referred to the web version of this article.)

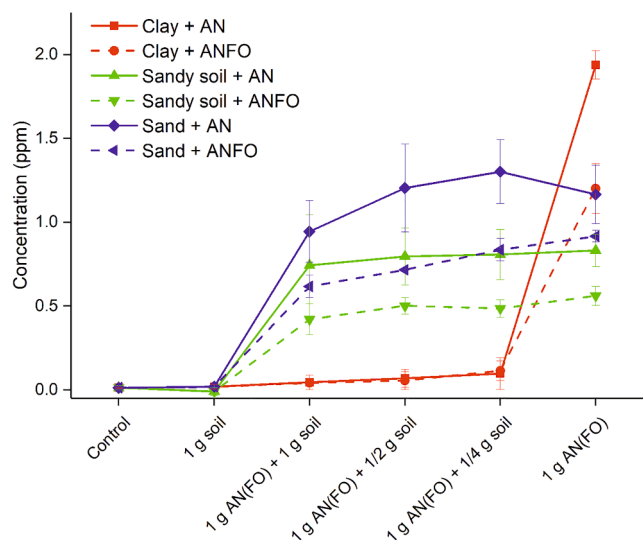


Fig. 4. Sensor responses to buried fertiliser and ANFO sample expressed in ppm NH_3 equivalent concentration. The AN(FO) samples were covered by 1, $\frac{1}{2}$, and $\frac{1}{4}$ g of clay, sandy soil, and sand. The results are averages of 3 measurements with freshly prepared samples and 2 different sensors. The error bars represent the standard deviation. Control experiments were conducted with an empty T-shaped sample holder.

not easily permeated by the vapour molecules emitted by the AN(FO) samples. The sand and sandy soil consist of larger particles and form a more porous layer, which is more permeable to the vapour molecules, resulting in a stronger sensor response.

The measured sensor responses are caused by unknown quantities of vapour emitted by the fertiliser and ANFO samples. However, because the response is caused by NH_3 , one of the decomposition products of ammonium nitrate, the sensors can be calibrated based on known NH_3 concentrations obtained through dilution with N_2 from a 10 ppm NH_3 in N_2 gas cylinder (BOC, UK). These calibrated sensors can then be used to determine the detected AN(FO) vapour concentration. For calibration, the sensors were exposed to 1–8 ppm NH_3 in N_2 for 5 min with a 15 min recovery time under N_2 . As expected, exposure to NH_3 causes a rapid and reversible increase in resistance. Furthermore, higher concentrations result in a larger sensor response (Fig. 3A). A linear fit based on 3 exposures per concentration was used as the calibration curve (Fig. 3B). The percentage resistance change, $\Delta R/R_0 \times 100\%$, was calculated with respect to the R_0 starting resistance at the start of each exposure. The calibration curve can also be used to calculate the limit of detection (LOD) of that particular sensor, defined as the gradient of the linear fit divided by 3 times the standard deviation of the baseline noise before the first exposure. The sensor shown in Fig. 3 has a limit of detection of 73 ± 11 ppbv. Calibrating each sensor against known NH_3 concentrations also allows us to account for differences between individual

sensors. These differences are inherent to sensors based on percolation networks. The large variations in the resistance caused by small variations in the network, even for sensors produced with the same parameters, are what give percolation network-based sensors their significantly improved sensitivity compared to more traditional thin film-based sensors.

Series of exposures like those shown in Fig. 2 were repeated 3 times for each combination of soil and AN(FO). The raw sensor responses were converted to equivalent NH_3 concentrations and the results are summarised in Fig. 4. The average detected concentrations range from 71 ± 52 ppbv, close to the LOD of 73 ± 11 ppbv, for the AN(FO) samples covered by 0.25–1 g clay to 1.94 ± 0.08 ppm for the strongest response to fertiliser without a soil layer. Fig. 4 shows that the sensor response to AN(FO) covered by clay is negligible, whereas AN(FO) covered by both sandy soil and sand give clear sensor responses. The response to AN(FO) covered by sand is stronger than that covered by sandy soil, which is consistent with sand being more permeable to the vapour emitted by AN(FO). As shown in Table 1, sand contains a larger fraction of larger particles than sandy soil, resulting in a more porous soil layer. Furthermore, Fig. 4 shows that in all instances AN causes a larger sensor response than ANFO. This is likely due to the diesel wetting both the soil layer and the crushed fertiliser granules, thereby decreasing the gas permeability of both the ANFO sample and the soil layer [16]. Fig. 4 also shows that the unconcealed AN(FO) at the end of the series of exposures to samples covered with clay gives a slightly stronger response than those at the end of series of exposures covered with sandy soil and sand. This is likely due to the sensor being more fully recovered before the exposure because the samples covered by clay released a smaller quantity of vapour compared to the samples covered by sandy soil and sand.

Conclusions

Buried fertiliser and ANFO samples were detected at sub-ppm concentrations using chemiresistive gas sensors based on percolation networks of PPy. Concealment under a layer of sand or sandy soil only slightly decreases the recorded sensor signal. On the other hand, clay effectively blocks the emitted vapour, resulting in an almost negligible sensor response. The soil type has a much larger impact on the sensor signal than the soil layer thickness.

It should be noted that due to safety considerations the fertiliser and ANFO samples were small and only weighed 1 g. In a real-life IED detection scenario the sample is likely to be at least 1 kg in mass and hence produce more vapour. However, the IED is also likely to be buried to a greater depth than in our study. How these factors affect each other will require further research in a dedicated secure environment. Furthermore, in future work environmental factors such as temperature, humidity, air instead of N_2 carrier gas, and the presence of other vapours should be taken into account by using an electronic nose-type setup and by recalibrating the sensor for real-world conditions.

Declaration of Competing Interest

The authors declare that they have no known competing financial interests or personal relationships that could have appeared to influence the work reported in this paper.

Acknowledgements

We are grateful to Professor Cesar Sierra for his advice. We thank Yara UK and Lisa Humphreys and Jeff Pons from Cranfield University for providing the fertiliser. For helpful discussions we also thank Krishnan Murugappan and Ben Armitage. This work was supported by the EPSRC Global Challenges Research Fund.

References

- [1] C. Kopp, Technology of improvised explosive devices, *Defence Today* 4649 (2008) 46–49.
- [2] F.L. Steinkamp, B. Giordano, G. Collins, S. Rose-Pehrsson, Volatile emissions of ammonium nitrate under flowing conditions, *Propellants Explos. Pyrotech.* 40 (5) (2015) 682–687.
- [3] J.C. Oxley, J.L. Smith, E. Rogers, M. Yu, Ammonium nitrate: thermal stability and explosivity modifiers, *Thermochim. Acta* 384 (2002) 23–45.
- [4] V.V. Hernandez, M.F. Franco, J.M. Santos, J.J. Melendez-Perez, D.R.d. Morais, W.F. d.C. Rocha, R. Borges, W. de Souza, J.J. Zacca, L.P.L. Logrado, M.N. Eberlin, D. N. Correa, Characterization of ANFO explosive by high accuracy ESI(±)-FTMS with forensic identification on real samples by EASI(–)-MS, *Forensic Sci. Int.* 249 (2015) 156–164.
- [5] J.M. Hendrickx, et al., Humanitarian IED clearance in Colombia, *SPIE Defense and Security Symposium* 6953 (2008) 9.
- [6] M.J. Lefferts, M.R. Castell, Vapour sensing of explosive materials, *Anal. Methods* 7 (21) (2015) 9005–9017.
- [7] M.K. Ram, O. Yavuz, M. Aldissi, NO₂ gas sensing based on ordered ultrathin films of conducting polymer and its nanocomposite, *Synth. Met.* 151 (2005) 77–84.
- [8] M.J. Lefferts, B.I. Armitage, K. Murugappan, M.R. Castell, PEDOT percolation networks for reversible chemiresistive sensing of NO₂, *RSC Adv.* 11 (37) (2021) 22789–22797.
- [9] Y. Wang, W. Jia, T. Strout, A. Schempf, H. Zhang, B. Li, J. Cui, Y.u. Lei, Ammonia Gas Sensor Using Polypyrrole-Coated TiO₂/ZnO Nanofibers, *Electroanalysis: An Int. J. Devoted Fundam. Pract. Aspects Electroanalysis* 21 (12) (2009) 1432–1438.
- [10] P.-G. Su, C.-T. Lee, C.-Y. Chou, Flexible NH₃ sensors fabricated by in situ self-assembly of polypyrrole, *Talanta* 80 (2) (2009) 763–769.
- [11] T.A. Ho, T.-S. Jun, Y.S. Kim, Material and NH₃-sensing properties of polypyrrole-coated tungsten oxide nanofibers, *Sens. Actuators, B* 185 (2013) 523–529.
- [12] S.J. Toal, W.C. Trogler, Polymer sensors for nitroaromatic explosives detection, *J. Mater. Chem.* 16 (2006) 2871–2883.
- [13] M.J. Lefferts, L.H. Humphreys, N. Mai, K. Murugappan, B.I. Armitage, J.-F. Pons, M.R. Castell, ANFO vapour detection with conducting polymer percolation network sensors and GC/MS, *Analyst* 146 (7) (2021) 2186–2193.
- [14] B.I. Armitage, K. Murugappan, M.J. Lefferts, A. Cowsik, M.R. Castell, Conducting polymer percolation gas sensor on a flexible substrate, *J. Mater. Chem. C* 8 (36) (2020) 12669–12676.
- [15] R.L. Van Dam *, B. Borchers, J.M.H. Hendrickx, Strength of landmine signatures under different soil conditions: implications for sensor fusion, *Int. J. Syst. Sci.* 36 (9) (2005) 573–588.
- [16] D. Benavente, J. Valdés-Abellán, C. Pla, E. Sanz-Rubio, Estimation of soil gas permeability for assessing radon risk using Rosetta pedotransfer function based on soil texture and water content, *J. Environ. Radioact.* 208–209 (2019) 105992, <https://doi.org/10.1016/j.jenvrad.2019.105992>.
- [17] S. Belkin, et al., Remote detection of buried landmines using a bacterial sensor, *Nat. Biotechnol.* 35 (2017) 308–310.
- [18] Y. Kabessa, et al., Standoff detection of explosives and buried landmines using fluorescent bacterial sensor cells, *Biosens. Bioelectron.* 79 (2016) 784–788.
- [19] R.N. Gillanders, I.D.W. Samuel, G.A. Turnbull, A low-cost, portable optical explosive-vapour sensor, *Sens. Actuators, B* 245 (2017) 334–340.
- [20] K. Murugappan, M.R. Castell, Bridging electrode gaps with conducting polymers around the electrical percolation threshold, *Electrochem. Commun.* 87 (2018) 40–43.
- [21] Rowland, J. & Mainiero, R. in *Proceedings of the Annual Conference on Explosives and Blasting Technique*. 163–174 (ISEE; 1999).
- [22] B. Zygumt, D. Buczkowski, Influence of ammonium nitrate prills' properties on detonation velocity of ANFO, *Propellants, Explosives, Pyrotechnics: An International Journal Dealing with Scientific and Technological Aspects of Energetic Materials* 32 (5) (2007) 411–414.
- [23] F.P. Shepard, Nomenclature based on sand-silt-clay ratios, *J. Sediment. Res.* 24 (1954) 151–158.